

Supporting Information for

High-Throughput Tumor-on-a-Chip Platform to Study Tumor-Stroma Interactions and Drug Pharmacokinetics

Chun-Wei Chi[†], Yeh-Hsing Lao[‡], Elizabeth C. Benoy[†], Chenghai Li[†], AH Rezwanuddin Ahmed[†], Zeynep Dereli-Korkut[†], Bingmei M. Fu[†], Kam W. Leong[‡] and Sihong Wang^{*†}

[†] Department of Biomedical Engineering, CUNY- The City College of New York, New York NY, 10031, USA

[‡] Department of Biomedical Engineering, Columbia University, New York, NY 10027, USA

* Corresponding author (shwang@ccny.cuny.edu)

This document includes

Materials and Methods

Figure S1. The correlation between RFP intensity and the MDA-MB-231 cell number

Figure S2. Representative images of the permeability measurement carried out in the device

Figure S3. Calibration between fluorescent intensities and the number of solute molecules

Figure S4. Permeability of hCMEC/D3 endothelium in the device

Figure S5. Time-lapse cell migration images in the *L*-TumorChip

Figure S6. Total numbers of cell aggregates formed in 8 chambers of the *L*-TumorChip over 7-day culture.

Figure S7. Caspase-3 activity observed in the bottom chamber of the *L*-TumorChip

Table S1. Bi-logistic fitted parameters for the Caspase-3 activity under doxorubicin treatment

Materials and Methods

Microfluidic device fabrication. We followed our previously published work to fabricate the device with minor modifications.^[1] Briefly, the SU8 master molds were made on the silicon wafer by photolithography with 150 μ m and 200 μ m height for the top channel and the bottom chamber, respectively. The SU8 pillars (70 μ m in height) were created for making holes on the middle membrane. Polydimethylsiloxane (PDMS, DOW Chemical, Midland, MI) was spin-coated and cured on the middle master for the thin membrane and directly casted on the masters for top and bottom layers. The bonding between layers was performed right after oxygen plasma treatment under a stereomicroscope (Motic).

Computational Fluid Dynamics Simulation. The flow pattern in *L*-TumorChip was simulated by using COMSOL 5.2a (Sweden). The Navier-Stokes equations with a laminar flow model were used for the free flow in the top channel and coupled with the standard Brinkman model for the porous region, the bottom chamber filled with Matrigel. The Free and Porous Media Flow module in COMSOL was used for the simulations. The inlet velocity boundary condition of the top channel was set to 100 μ m/s, which was in the range of velocity in human capillary, and the hydraulic permeability of 2×10^{-14} m² of a 4 mg/mL Matrigel was used for the bottom chamber. The pressure at outlet of top channel was set to zero. The rest of boundaries were identified as impermeable wall with a no-slip condition.

Cell culture. Human breast cancer cell line MDA-MB-231 (HTB-26TM) and human normal fibroblast CCD-1096Sk (CRL-2129) were purchased from American Type Culture Collection (Manassas, VA). MDA-MB-231 and normal fibroblast were cultured in high glucose DMEM (Thermo Fisher, Waltham, MA) and Minimum Essential Medium (Thermo Fisher), respectively,

supplemented with 10% Fetal Bovine Serum (FBS; Atlanta Biologicals, Atlanta, GA) and 1× penicillin-streptomycin (Thermo Fisher). Human dermal blood microvascular endothelial cell (HMVEC) was cultured in the EGMTM-2 basal medium supplemented with growth factors (Lonza, Switzerland). Human mesenchymal stem cells (MSCs) were cultured in low glucose DMEM (Thermo Fisher) supplemented with 10% FBS and 1× penicillin-streptomycin, and the seeding density of each subculture was 5000 cells/cm².

3D coculture in the microfluidic device. The microfluidic device was firstly UV sterilized in cell culture hood for at least 1h. In order to enhance cell attachment, fibronectin bovine plasma (30 µg/mL; Sigma-Aldrich, St. Louis, MO) was introduced into the device immediately after oxygen plasma treatment. The device was then incubated at 37 °C for another 1h filled with the complete medium. After the pretreatment, the device was cooled down in the refrigerator. Cancer cells or the mixture of cancer cells and stromal cells (1:1) at a concentration of 2×10⁷ cells/mL were mixed in 4 mg/mL growth factor reduced Matrigel (Corning, Corning, NY), and subsequently the cell-containing Matrigel was loaded into the bottom chamber. Inlets and outlets of the top channel were clamped during the cell seeding process so that there was no pressure gradient, which could prevent crosstalk between the top channel and the bottom chamber. After gelation at 37°C for 1h, the clamped top channel was released and, reversely, inlets and outlets of the bottom chamber were clamped. The fresh medium was then continuously introduced into the top channel using a syringe pump with a speed of 100 µm/s. As shown in **Figure 1B** for the fluid flow profile in our *L*-TumorChip, the medium support to cells in the bottom chamber was from the top channel through the pores in the middle layer by diffusion and slow convection mimicking interstitial flow. The device was incubated at 37°C for overnight under 5% CO₂ atmosphere. Afterwards, HMVEC was

seeded to the top channel with a density of 1×10^7 cells/mL. Excess HMVECs were removed at 1 h post-seeding. Similarly, after seeding, the device was incubated at 37°C for under 5% CO₂ atmosphere; continuous medium flow was given after HMVEC attached to the channel (at ~6 h post-seeding). A combinational medium composed of EGMTM-2MV, DMEM, and EMEM in a ratio of 1:1:1 was used throughout all of our culture conditions. The ratio was determined based on the ratio of endothelial cells, cancer cells and fibroblasts used in our coculture conditions, and we did not observe any deteriorate effects on the cells when using this medium recipe.

Immuno-characterization of endothelial cells in the microfluidic device. To characterize endothelial cells in the device, GFP- or RFP-expressing MDA-MB-231 was used and HMVECs were stained with CD31 (mouse monoclonal clone 89C2; Cell Signaling Technology, Danvers, MA) or VE-cadherin (rabbit monoclonal clone D87F2; Cell Signaling Technology) antibodies plus its paired fluorescence-labeled secondary antibodies, Alexa Fluor 594-labeled goat anti-mouse IgG (Thermo Fisher) or Alexa Fluor 488 Goat anti-rabbit IgG (Thermo Fisher). At 24 h post-seeding, cells in the device were fixed with 4% paraformaldehyde (Thermo Fisher) for 60 min and permeabilized with 0.2% Triton X-100 (Thermo Fisher) for 10 min. Afterwards, it was blocked in PBS containing 3% Bovine serum albumin (Sigma-Aldrich, St. Louis, MO) and 0.3% Triton X-100 for 1h. For endothelium staining, the device was incubated with the primary antibodies at 4°C for overnight and then incubated with secondary antibodies at room temperature (RT) for 2h. Washes with PBS were carried out between steps. Nuclei were also stained with Hoechst 33342 (Thermo Fisher). The endothelium layer of the device was then visualized using a confocal microscope (Zeiss LSM800, Germany).

Vascular permeability measurement. The diffusive permeability of endothelium was characterized using two different molecular weights of dextran, 10 kDa FITC-labeled dextran and 70 kDa Texas Red-labeled dextran (Thermo Fisher). One unit of the microfluidic device was set up in the side-view under fluorescence microscope (Zeiss AxioObserver Z.1; see **Figures 1B** and **S2** for details). Time-lapse images were acquired every 0.3s. Because the measurement was based on an assumption that the change of fluorescent signals correlated with solute's concentration, the dextran's concentration would need to be within the linear detection range of the microscope. Prior to the permeability measurement, the calibration between concentration and intensity of fluorescence-tagged dextran in the measuring window was confirmed under the same setting (fixed exposure time) for each type of dextran. As shown in **Figures S3(A)-(C)**, 0.1 mg/mL sodium fluorescein, 0.6 mg/mL 10 kDa FITC-dextran and 0.6 mg/mL 70kDa Texas Red-dextran were used for permeability measurement. In addition, the depth of light collection was also calibrated by measuring intensity of fixed amount of fluorescent molecule in different depths of the chamber as the other work reported.^[2] Different concentrations of 10 kDa FITC-dextran were loaded into chambers with various depths (110, 140, 210 and 420 μm) to get each chamber containing the fixed amount of fluorescent molecule. As shown in **Figure S2(D)**, the intensity with the increase of chamber depth throughout the range implied the depth limit for light collection our system is below 140 μm . As a result, the permeability could be estimated by the following equation.^[3]

$$P = \frac{1}{\Delta I_0} \left(\frac{dI}{dt} \right)_0 \frac{V}{A} \quad (\text{Eq. S1})$$

where I and ΔI_0 represented the fluorescent signal and initial intensity in the filled top channel, respectively. V was the volume of the lumen, and A was the area, which solute flew across from lumen to the tissue side. Based on the size of measuring window, the depth of collected light and

the geometry of device, the sampled region was a cuboid. Therefore, V/A was equal to the height of the top channel in this system.

Migration. Prior to the study, HMVEC was stained with a long-term fluorescent dye, PKH67 cell linker kit (Sigma-Aldrich), following the manufacturer's instructions. Additionally, RFP-expressing MDA-MB-231 was seeded in the device. After a 7-day culture, the 3D sliced fluorescent images were captured by the confocal microscope (Zeiss LSM 880). The maximum projection was performed to reconstruct the 3D images.

Cancer-associated fibroblast-like differentiation of MSCs: Following the previously reported methods,^[4] we differentiated MSCs to cancer cell-associated fibroblast (CAF) by culturing them with the MDA-MB-231-conditioned media. In order to generate conditioned media, MDA-MB-231 was cultured to a confluency of 70-90% and then incubated with fresh medium (DMEM with 10% heat-inactivated FBS and 1% PS) at 37°C under 5% CO₂ atmosphere overnight. The collected conditioned medium was then centrifuged at 3000 rpm for 5 min and filtered by a 0.22µm filter to remove cell debris. During the differentiation process, the conditioned medium was changed every three days, and the MSCs were subcultured when the confluency approached ~80%. Untreated MSCs were also cultured under the same conditions as a control for the entire process. Afterwards, the cells cultured with and without conditioned media were then characterized by immunofluorescence staining and flow cytometry analysis. Immunofluorescence staining was conducted as aforementioned.

Growth of cancer cells in device. The effect of different stromal cells (normal fibroblast, MSC and CAF) on cancer growth was evaluated by monitoring fluorescent signal of GFP-expressing MDA-MB-231. The stromal cell was co-cultured with MDA-MB-231 (1:1) in 4 mg/mL Matrigel in the bottom chamber. The seeding concentration of cancer cells was 2.5×10^6 cells/mL for all groups. The stacked fluorescent images were captured by Zeiss AxioObserver, slicing the entire bottom chamber with a $4\mu\text{m}$ interval at days 0, 2, 4, 6 and 8 post-seeding. Fluorescent signal of each image was added up after background subtraction for each chamber and normalized to that at day 0. Four chambers were randomly chosen for each condition to show the variation.

Drug response in the microfluidic device. The caspase-3 activity was monitored during doxorubicin treatment using Biotium NucView®488 Caspase-3 enzyme substrate (Fremont, CA). At 24h post-HMVEC seeding, the device was set up in the on-stage incubator at 37°C under 5% CO_2 atmosphere on the microscope. The caspase-3 substrate ($3\mu\text{M}$) in the medium with or without $4\mu\text{M}$ doxorubicin was given to the device continuously using a multichannel syringe pump with a speed of $100\mu\text{m/s}$. The Z-stacked images were captured in a 2h interval for 48h. The intensity of entire stacked images at each location was added up after background subtraction and normalized to T_0 (before drug treatment). A bi-logistic model was applied for curve fitting through a non-linear least squares approach implemented by MATLAB R2018a (MathWorks, Natick, MA):

$$\frac{dS(t)}{dt} = a_1 S(t) \left(1 - \frac{S(t)}{k_1}\right) + a_2 S(t) \left(1 - \frac{S(t)}{k_2}\right) \quad (\text{Eq. S2})$$

The model comprises two phases of logistic function, and the solution was given in Eq (1) of the main text.

Statistical Analysis. Data are presented as the mean \pm standard deviation. One-way/two-way ANOVA followed by Tukey's Multiple Comparison Test or Student t-test was performed using GraphPad Prism 5.01 (GraphPad Software, San Diego, CA). Statistical significance was defined as * ($p < 0.05$), **, ($p < 0.01$) or *** ($p < 0.001$). Sample size and analysis method used were described in each figure legend.

Supplementary Figures

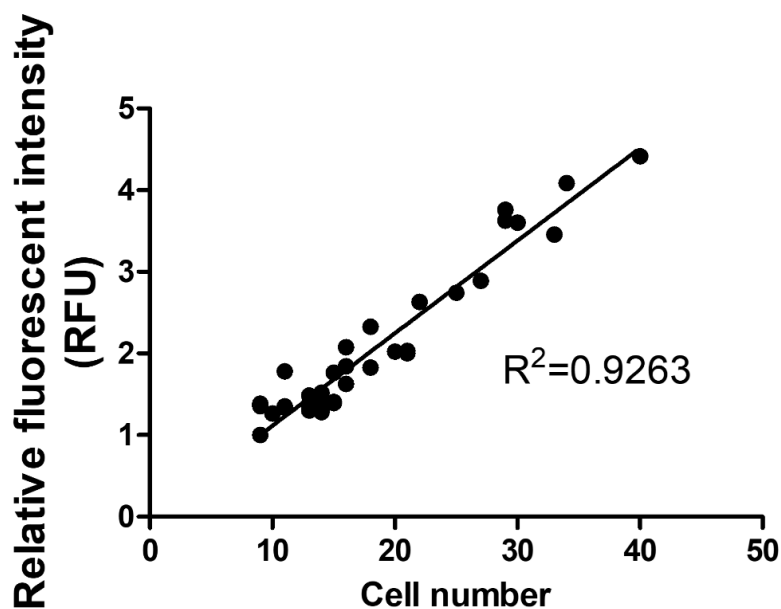


Figure S1. The correlation between fluorescent intensity and the number of RFP-expressing MBA-MD-231. Each dot represents a region with defined cell number from the sliced images taken in the device.

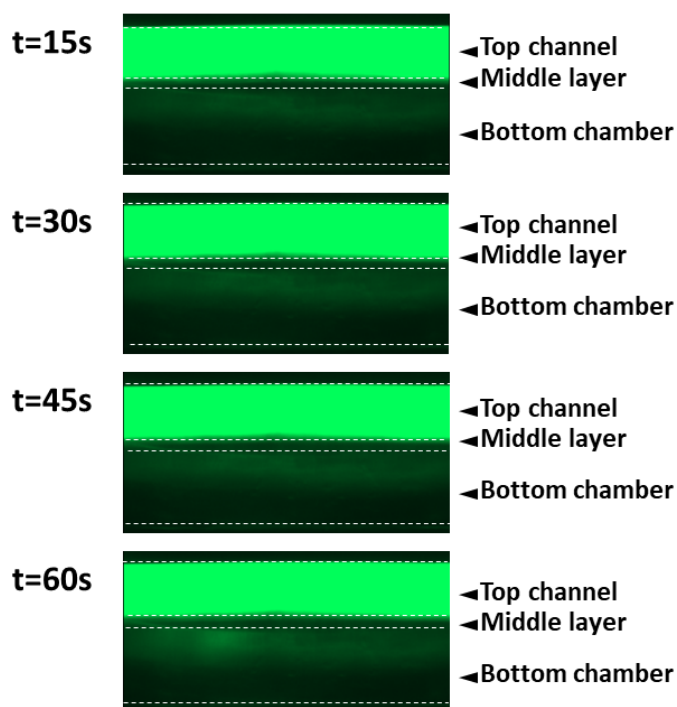


Figure S2. Representative images of the permeability measurement carried out in the device.

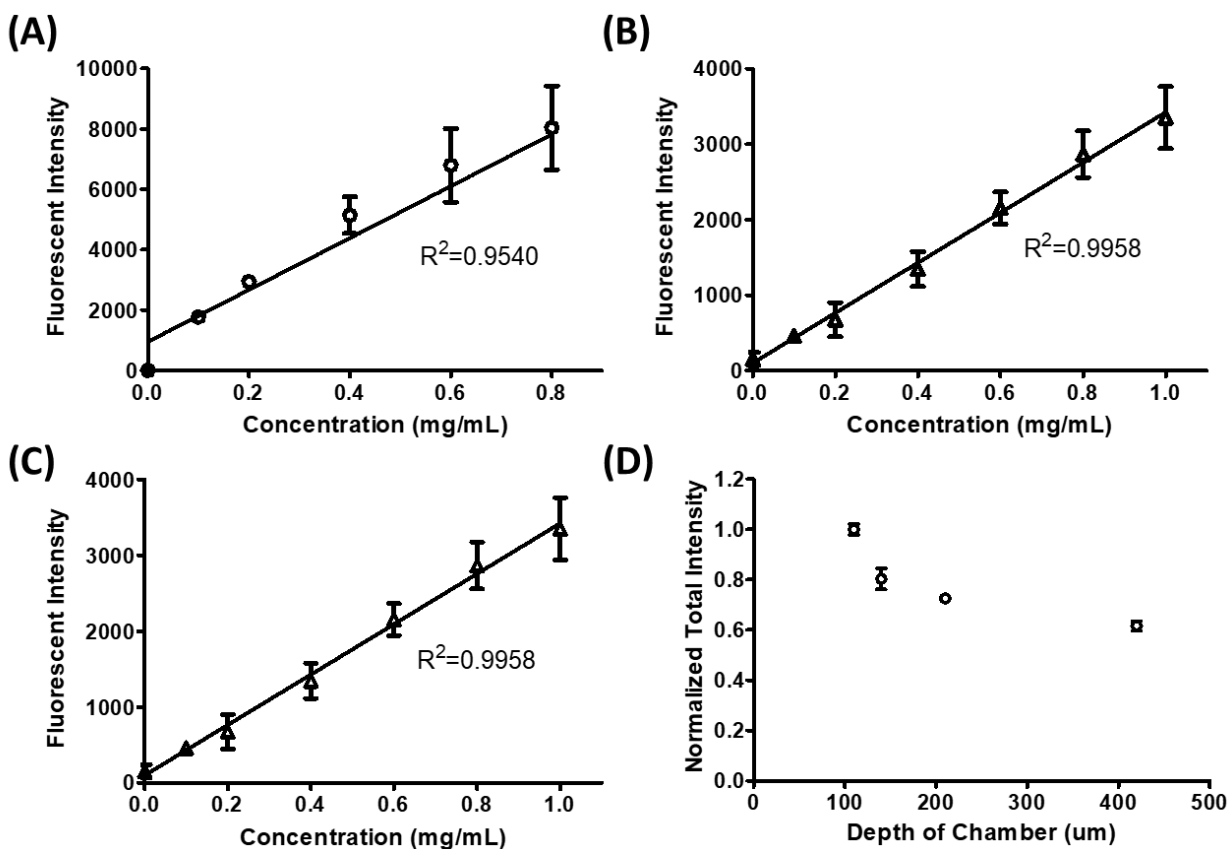


Figure S3. Calibration between fluorescent intensities and the number of solute molecules. Calibrations with (A) sodium fluorescein (B) 10 kDa FITC-dextran (C) 70 kDa Texas Red-dextran. (D) Depth of light calibration under 10 \times fluorescent microscope (Zeiss AxioObserver, Germany). Results are presented as average \pm standard deviation (S.D., $n = 4$).

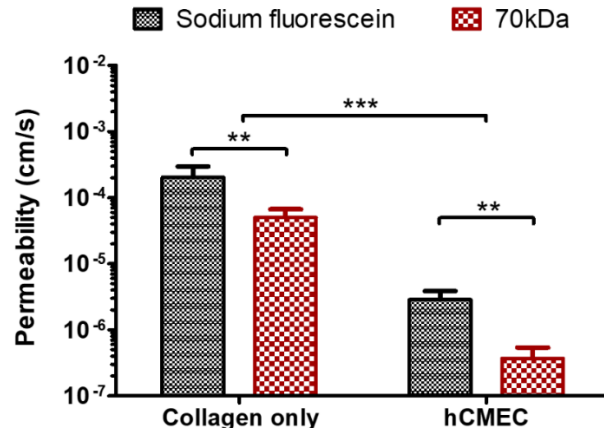


Figure S4. Permeability of hCMEC/D3 endothelium in the device (bottom chamber filled with collagen). Results are presented as average \pm S.D. ($n = 4$). Significance was determined using 2-way ANOVA with Tukey's Multiple Comparison Test (**, $p < 0.01$; ***, $p < 0.001$).

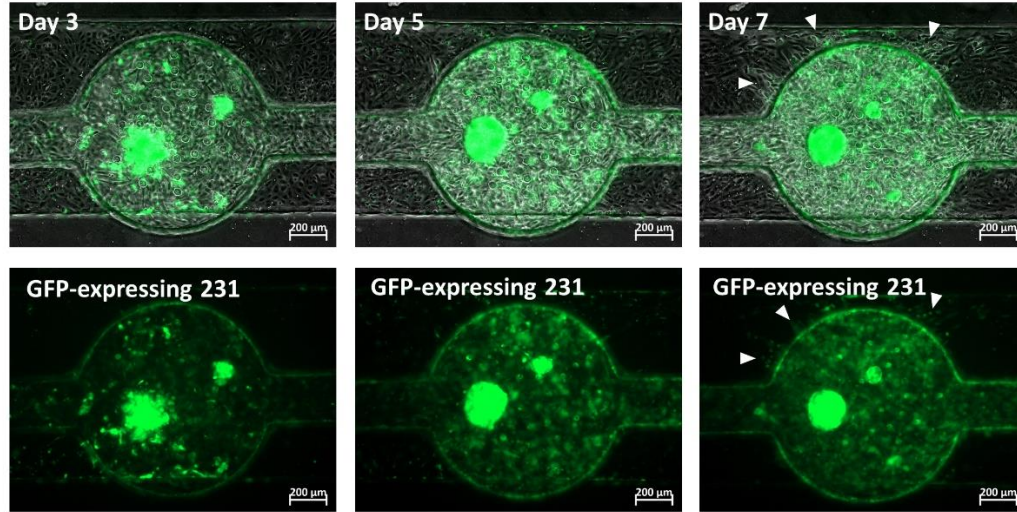


Figure S5. Time-lapse cancer cell migration images in the *L*-TumorChip. Images were taken using the wide-field fluorescence microscope (Zeiss AxioObserver Z.1). White arrows point to migrated cancer cells from the bottom round chamber to the top channel obviously indicated by their locations.

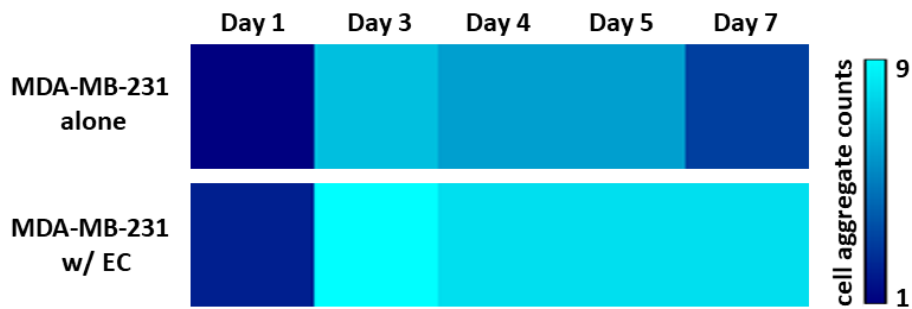


Figure S6. Total numbers of cell aggregates formed in 8 chambers of the *L*-TumorChip over 7-day culture.

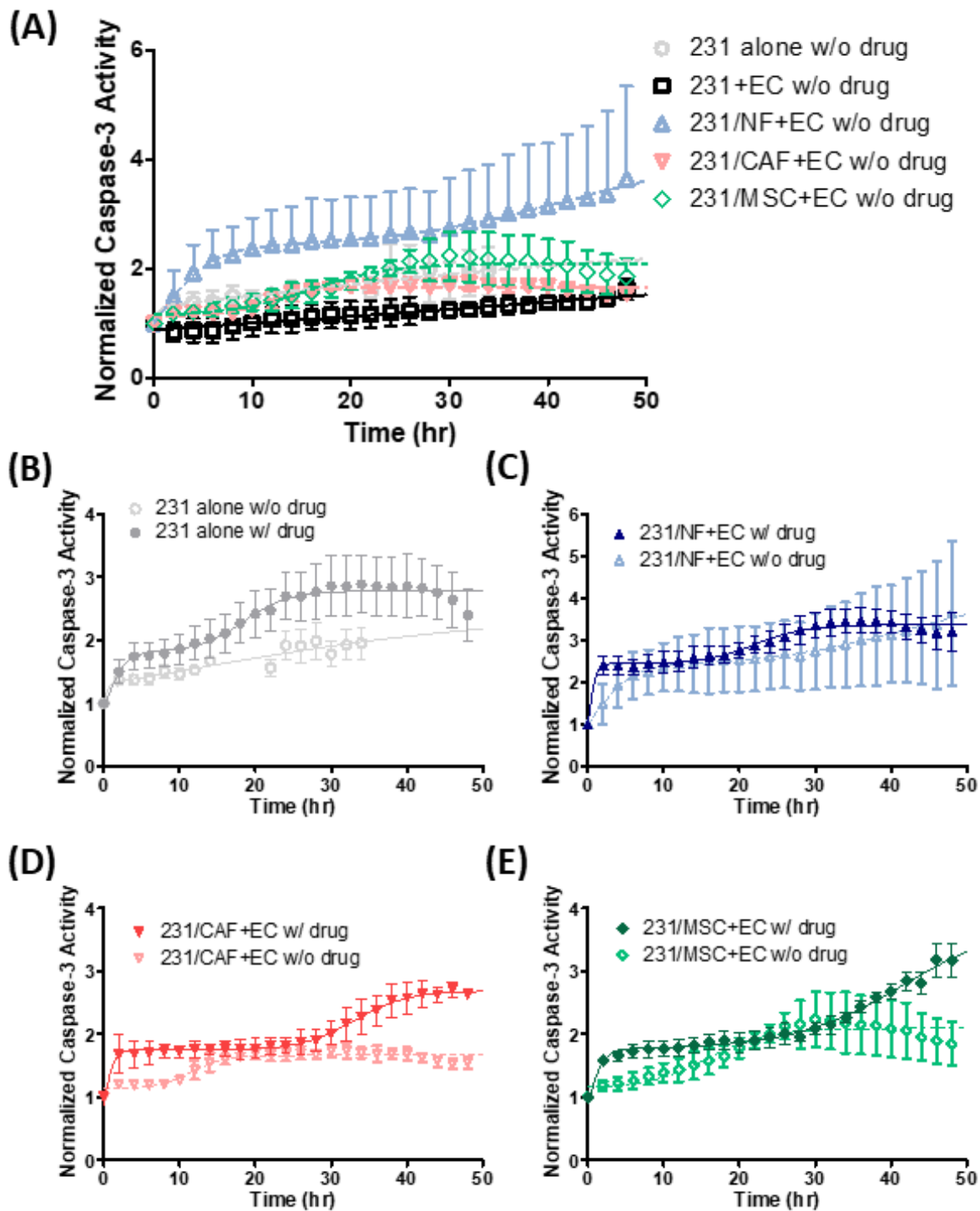


Figure S7. Caspase-3 activity observed in the bottom chamber of the *L*-TumorChip. (A) Comparison of different microenvironments without drug treatment. Comparisons between drug and no drug treatment in (B) cancer cell alone condition, coculturing with (C) normal fibroblasts, (D) CAFs and (E) MSCs. Results are presented as average \pm S.D. ($n = 3$).

Table S1. Bi-logistic fitted parameters for the Caspase-3 activity under doxorubicin treatment

	k_1	a_1	b_1	k_2	a_2	b_2	k_1+k_2	R^2
231 alone	1.82	0.75	2.32×10^{-6}	0.96	0.34	18.44	2.78	0.96
231+EC	1.99	1.22	1.97×10^{-12}	0.51	0.33	22.56	2.50	0.95
231/NF+EC	2.44	2.21	0.17	0.92	0.30	22.12	3.36	0.98
231/CAF+EC	1.75	1.57	2.22×10^{-14}	0.94	0.28	33.02	2.69	0.99
231/MSK+EC	1.77	0.98	2.22×10^{-14}	2.05	0.14	41.72	3.81	0.99

References

- [1] Z. Dereli-Korkut, H. D. Akaydin, A. H. R. Ahmed, X. J. Jiang, S. H. Wang, *Anal Chem* **2014**, 86, 2997.
- [2] W. Yuan, Y. Lv, M. Zeng, B. M. Fu, *Microvasc Res* **2009**, 77, 166.
- [3] V. H. Huxley, F. E. Curry, R. H. Adamson, *Am J Physiol* **1987**, 252, H188.
- [4] a) P. J. Mishra, P. J. Mishra, R. Humeniuk, D. J. Medina, G. Alexe, J. P. Mesirov, S. Ganesan, J. W. Glod, D. Banerjee, *Cancer Res* **2008**, 68, 4331; b) L. Shangguan, X. Ti, U. Krause, B. Hai, Y. Zhao, Z. Yang, F. Liu, *Stem Cells* **2012**, 30, 2810.